

Sticking Lifetime of Ultracold CaF Molecules in Triplet Interactions

Published as part of *The Journal of Physical Chemistry virtual special issue "Cold Chemistry"*.

Dibyendu Sardar and John L. Bohn*



Cite This: *J. Phys. Chem. A* 2023, 127, 4815–4821



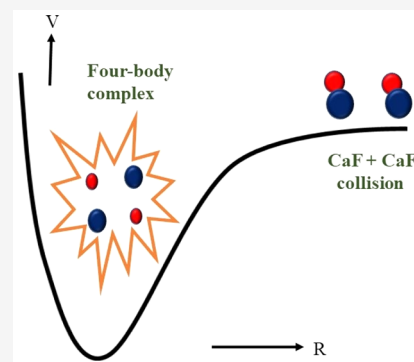
Read Online

ACCESS |

Metrics & More

Article Recommendations

ABSTRACT: A six-dimensional potential energy surface is constructed for the spin-polarized triplet state of CaF–CaF by *ab initio* calculations at the CCSD(T) level of theory, followed by Gaussian process interpolation. The potential is utilized to calculate the density of states for this alkaline-earth-halogen system where we find the value $0.038 \mu\text{K}^{-1}$, implying a mean resonance spacing of $26 \mu\text{K}$ in the collision complex. This value implies an associated Rice–Ramsperger–Kassel–Marcus lifetime of $1.8 \mu\text{s}$, thus predicting long-lived complexes in collisions at ultracold temperatures.



INTRODUCTION

The encounter between two CaF molecules, both in their ${}^2\Sigma$ ground state, can proceed through either singlet or triplet interactions of the four-body system Ca_2F_2 . In a previous paper,¹ we developed the singlet scattering surface for this system, identifying the reaction $2\text{CaF} \rightarrow \text{CaF}_2 + \text{Ca}$ as barrierless and exothermic by $\sim 4300 \text{ cm}^{-1}$. Thus, CaF molecules that are not spin-polarized may be expected to encounter one another on this surface and quickly undergo chemical reactions.

By contrast, spin-polarized CaF molecules will initially meet only on the triplet surface, which, as we will show below, cannot lead directly to chemical reactions in low-temperature gases. If this polarization is maintained, that is, to the extent the molecules interact only via the triplet surface, they will not react. Reaction may, however, occur due to spin–orbit or other couplings to the singlet state, which, as we have shown previously,¹ is reactive. The triplet surface is therefore an important starting point for understanding ultracold reactions of this radical, and we construct such a surface in this article.

Even if they are restricted to the triplet surface, spin-polarized CaF molecules may not scatter elastically in a simple way. At ultracold temperatures, diatomic molecules are often observed to vanish into long-lived complex states, a phenomenon known as “sticking”.² Long dwell times in this complex can not only appear as a loss mechanism, they can also enhance even weak couplings to the singlet surface, thereby further reducing the immunity of spin-polarized CaF molecules to reaction. The sticking time, i.e., the lifetime of the collision complex is associated with the Rice–Ramsperger–

Kassel–Marcus (RRKM) formalism, which assumes ergodic dynamics. In this paper we therefore use the triplet surface to estimate this lifetime in the RRKM approximation, finding it to be $1.8 \mu\text{s}$.

AB INITIO METHOD OF CALCULATION

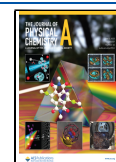
The *ab initio* electronic structure calculations are performed using the MOLPRO 2012.1 software package.³ The calculations start by first computing spin-restricted Hartree–Fock (RHF) wave functions. Thereafter, the RHF wave functions are used as an initial guess for the next coupled-cluster calculations including single, double, and perturbative triple excitation [CCSD(T)] calculation. This approach is favorable for the short-range physics considered, can be described by a single determinant, and is better applicable to the nonreactive triplet surface of CaF–CaF than the multi reference configuration interaction (MRCI) method.

The ground state of a Ca atom possesses two valence electrons in the 4s atomic orbitals and eight subvalence electrons in the 3s3p orbitals. We correlate only the outer core electrons 4s of Ca, and therefore, we consider a pseudopotential based correlation-consistent polarized weighted core valence triple- ζ basis set cc-pw-CVTZ-PP.⁴ The inner core

Received: March 12, 2023

Revised: May 11, 2023

Published: May 25, 2023



electrons are replaced by an effective core potential ([ECP10MDF])⁵ of the Stuttgart/Koeln group. By contrast, we use the aug-cc-PVTZ⁶ basis set for the atom F which is a correlation-consistent valence triple- ζ basis and belongs in the augmented class to treat 2s2p electrons explicitly where the 1s electrons of F remain uncorrelated. We do not correct for the basis set superposition error and the justification is given in the next following section.

Diatomic Species. First, we study the relevant diatomic species CaF, Ca₂, and F₂ to verify our current method of calculation and the used basis sets. Table 1 compares the

Table 1. Optimized Molecular Parameters of CaF, F₂, and Ca₂ Including Equilibrium Bond Lengths (r_e , Bohr) and Depth of the Well (D_e , in cm⁻¹)

system	symmetry	r_e	D_e
CaF		3.70	43614
theory ⁷	² Σ	3.69	44203
expt ⁸		3.71	
F ₂		2.68	12738
theory ⁹	¹ Σ	2.66	12880
expt ¹⁰		2.67	13410
Ca ₂		8.20	1097
theory ¹¹	¹ Σ	8.08	1102
expt ¹²		8.09	1075 ± 150

diatomic properties in terms of the equilibrium bond length (r_e) and depth of the well D_e to previously reported theoretical and experimental results. In this table, we show the results of our RHF-CCSD(T) calculations. All the bond lengths are expressed in Bohr and the well depths are in cm⁻¹. The experimental uncertainties are given for those where the values are reported. From Table 1 it is clear that the equilibrium bond length for each of the diatomic systems is in agreement with the literature value with an uncertainty less than 1% and we accept this as adequate. However, our method underestimates the depth of the well by ~500 cm⁻¹ for both CaF and F₂ molecular systems. Therefore, we consider this to estimate the uncertainty in our current method of calculations. The adequacy of the basis set is discussed below in the context of the four-body surface.

Energies of the Possible Asymptotes. Here we discuss the energies of the various dissociation possibilities with respect to the asymptotic energy of triplet CaF–CaF. There are four possible asymptotes that need to be considered in the domain of cold collisions between two calcium monofluoride molecules on the triplet surface. These asymptote are Ca₂ + F₂, Ca₂F + F, CaF₂ + Ca, and CaF + CaF. The energies of these possible asymptotes are tabulated in Table 2 where the zero of

Table 2. Energy of the Four Possible Asymptotic Arrangements with the Associated Symmetries Is Considered^a

asymptotic arrangements	symmetry	energy (cm ⁻¹)
CaF + CaF	² Σ + ² Σ	0
Ca ₂ + F ₂	¹ Σ + ¹ Σ	+73653
Ca ₂ F + F	² B + ² P	+34483
CaF ₂ + Ca	¹ A' + ¹ S	-4922
CaF ₂ + Ca	³ A" + ¹ S	+10313

^aThe zero of the energy is considered at CaF–CaF asymptote.

the energy is set at CaF + CaF asymptote. We find that the asymptotes Ca₂ + F₂ and Ca₂F + F lie 73653 and 34483 cm⁻¹ above the incident CaF + CaF asymptote and are therefore energetically inaccessible at low collision energies.

On the other hand, for the dissociation channel CaF₂ + Ca, there are two possible asymptotes. The asymptote having symmetry (³A" + ¹S) lies 10313 cm⁻¹ above the CaF + CaF asymptote and is inaccessible. By contrast, the CaF₂ + Ca asymptote is lower in energy but possesses singlet symmetry, irrelevant to direct reaction on the triplet surface. From these considerations, we conclude that the triplet surface is nonreactive.

Four-Body Surface. Construction of the potential energy surface of the four-atom CaF–CaF system is performed in two steps. Initially, an *ab initio* calculation is carried out, as described above, on a selected grid of atomic coordinates. The surface at other configurations, where the *ab initio* calculation was not performed, is estimated using Gaussian Process (GP) interpolation. To this end, the coordinates of the atoms are cast in Jacobi coordinates ($R, r_{13}, r_{24}, \theta_1, \theta_2, \phi$) as shown in Figure 1, where R is the center of mass (CM) distance between two CaF molecules, r_{13} (r_{24}) is the monomer bond length of CaF, θ_1 (θ_2) is the polar angle, and ϕ is the dihedral angle.

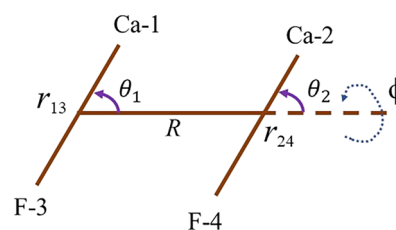


Figure 1. Coordinates for the asymptotic arrangement CaF–CaF in Jacobi coordinates. The numbers 1–4 represent the labeling of the concerned atoms Ca and F.

As a first step, we calculate global and local minima geometries of the triplet surface of the Ca₂F₂. This is accomplished by geometry optimization method using the relevant MOLPRO subroutine, and these calculations are done in the RHF-CCSD(T) level of theory with the basis sets described above. We find one global minimum and one local minimum having symmetries D_{2h} and C_s , respectively. The depth of the well (D_e) for the global minimum is 18074 cm⁻¹ whereas for the local minimum $D_e = 8760$ cm⁻¹, relative to the CaF + CaF asymptote. The geometrical parameters and the D_e 's are tabulated in Table 3.

In Table 3 we present the optimized bond lengths and optimized energies for the two minima of the singlet surface¹ in addition to the triplet surface, to make a comparison. We note that singlet and triplet surfaces both are minimized at nearly the same geometry and have essentially the same energy, with the singlet being only 849 cm⁻¹ deeper.

Qualitatively, the similarity in minima can be seen as follows. Electrons migrate in the four-atom system so that the two F atoms are essentially closed-shell F⁻ ions, while the positive Ca ions each have spin 1/2. The singlet and triplet states of the pair of Ca ions would normally be expected to differ in energy, as the molecular orbital in the coordinate between them would be symmetric (and bonding) for the singlet state, antisymmetric (and antibonding) for the triplet state. However, in the D_{2h} equilibrium geometry, the Ca ions are a distance of 6.4 a_0 apart, whereby both orbitals are near zero in the middle, hence

Table 3. Energy of the PES Ca_2F_2 (cm^{-1}) for the Global and Local Minima with Optimized Bond Lengths (Bohr)^a

surface	symmetry	r_{12}	r_{13}	r_{34}	r_{23}	r_{24}	r_{14}	E_{min}
singlet	D_{2h}	6.360	4.057	5.039				-18923
triplet		6.402	4.065	5.013				-18074
singlet	C_s	6.522	3.756	7.337	4.076	4.007	10.268	-15363
triplet		7.035	3.765	7.144	4.120	3.949	10.628	-8760

^aThe energies are referred to the $\text{CaF} + \text{CaF}$ dissociation threshold.

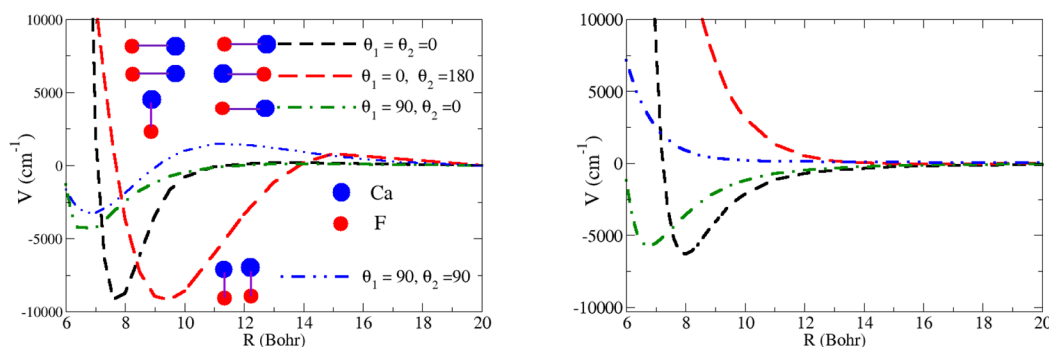


Figure 2. Variation of energies for the geometries head-tail, head-head, and T-shaped are shown in the left- and right-hand panels for the singlet and triplet surfaces of CaF-CaF , respectively. Blue and red circles represent the atoms Ca and F.

minimizing the distinction between bonding and antibonding orbitals.

Finally, we compare the singlet and triplet surfaces of CaF-CaF in CCSD(T) level of theory for some particular geometries, namely, head-tail ($\theta_1 = 0, \theta_2 = 0$), head-head ($\theta_1 = 0, \theta_2 = \pi$), T-shaped ($\theta_1 = \pi/2, \theta_2 = 0$), and parallel geometry ($\theta_1 = \pi/2, \theta_2 = \pi/2$) of the CaF-CaF . In the left-hand panel (LHP) of Figure 2, we present the variation of energy of CaF-CaF for the singlet state as a function of R (the distance between two centers of mass of CaF-CaF) for head-tail (black), head-head (red), T-shaped (green), and parallel (blue) geometries. The blue and red circles represent the atoms Ca and F, respectively. Potential curves for the same geometries are plotted in the right-hand panel (RHP) for the nonreactive triplet surface. Since CaF is a polar molecule having permanent dipole moment ~ 3.05 D,⁷ at the vary largest separations R , the interaction is primarily that of two dipoles. In this regime, molecules in the head-to-tail orientation (black) are attractive at long-range. For both singlet and triplet potentials, this attraction continues to much shorter range, before ultimately turning around and giving strong intermolecular repulsion at small R . Molecules meeting in T-shaped (green) and side-by-side (blue) geometries will experience repulsive dipole-dipole interactions at large R . Yet on the scale shown, they deviate from one another, with the side-by-side arrangement proving repulsive over most of the range of R shown. This geometry, in fact, never becomes attractive in the triplet surface.

Finally, the head-to-head geometry (red) shows strong repulsion due to dipolar interactions at long-range. It is here that the greatest difference between singlet and triplet potentials occurs. The singlet surface reaches a quite deep minimum at $R = 9.2$, while the triplet surface remains repulsive for all values of R . This is as expected for the close approach of the essentially spin-1/2 Ca^+ ions, with the F^- atoms behaving as spectators.

BASIS SET EXTRAPOLATION

Here we discuss the quality of our chosen basis set. To this purpose, we compare the global well depth obtained for our standard basis set for Ca (cc-pw-CVTZ-PP) to the other two correlation consistent basis sets having higher and lower angular momentum compared to the basis cc-pw-CVTZ-PP. The basis set of F = aug-cc-PVTZ is assumed to be the same for this calculation. We find that the correlation consistent basis having higher angular momentum of Ca (cc-pw-CVQZ-PP) offers the depth of the well 17992 cm^{-1} for the global minimum, in agreement with our standard basis set for Ca as shown in Table 3. However, the depth of the well becomes 5% uncertain concerning another tested basis set of Ca = cc-pw-CVDZ-PP. Therefore, DZ basis set of Ca is not enough to calculate the complete surface.

Next, we make a quantitative estimation to verify further the quality of the used basis sets both for Ca and F in terms of the complete basis set (CBS) extrapolation. The CBS extrapolation scheme is quite useful for large correlation- or polarization-consistent basis sets. The larger the basis sets we use, the more accurate the estimate of the CBS limit we will obtain. Basis set extrapolations are most important for highly correlated electronic structure methods, where basis set effects are large and often quite systematic in nature, and where calculations with large basis sets are often prohibitively expensive.

Here we perform the extrapolation for the two basis sets, identified by whether they include triple (TZ, $n = 3$) or else quadruple (QZ, $n = 4$) excitations to explore the CBS limit. This basis set extrapolation provides an accurate estimate for the CBS limiting energy, which by definition has zero basis set superposition error (BSSE). Several formulas have been used for extrapolating finite basis set results to the complete basis set limit. An accurate and robust extrapolation function is given by

$$E_n = E_{\text{CBS}} + A(n + 1/2)^{-4} \quad (1)$$

where A is a fitting coefficient and $n = 3$ or 4 as indicated above. To estimate the CBS energy, we consider TZ basis both

for Ca = cc-pw-CVTZ-PP and F = aug-cc-PVTZ, and we use the basis sets cc-pw-CVQZ-PP and aug-cc-PVQZ for Ca and F as QZ basis. If we solve two equations obtained from eq 1, one for $n = 3$ and one for $n = 4$, and eliminating A , then the CBS energy value becomes

$$E_{CBS} = 1.5772E_{QZ} - 0.5772E_{TZ} \quad (2)$$

Here, E_{nZ} represents the energy corresponding with the basis sets nZ ($n = 3, 4$) for a particular geometry. We estimate the E_{CBS} limiting energy -17974 cm^{-1} for the global minimum of the triplet CaF–CaF surface. Therefore, the difference in energy between the depth of the well for the TZ basis concerned with Ca and F and E_{CBS} is approximately 100 cm^{-1} . Thus, we conclude that the TZ basis set of Ca and F is adequate for calculating the complete potential energy surface of CaF–CaF.

GAUSSIAN PROCESS REGRESSION

Machine learning (ML) is a powerful tool for interpolating multidimensional potential energy surfaces. One of the most familiar approaches to building interpolation of models is Gaussian Process regression, which is a nonparametric kernel-based probabilistic ML algorithm including Bayesian information criterion.^{13,14}

For interpolation purposes, we convert atomic coordinates from their original Jacobi coordinates to inverse-atomic-distance coordinates. Each set of six such coordinates is denoted by the six-dimensional vector \mathbf{x}_i . Thus, the total data set, for N configurations at which the energy is computed, is denoted as $\mathbf{x} = (\mathbf{x}_1, \mathbf{x}_2, \dots, \mathbf{x}_N)^T$. The *ab initio* energies are given by \mathbf{y} for each \mathbf{x}_i . The GP model is trained by \mathbf{x} , and the prediction of the energy as a normal distribution at an arbitrary point \mathbf{x}_* is perceived by a mean (μ) and standard deviation (σ) having the following form

$$\mu(\mathbf{x}_*) = K(\mathbf{x}_*, \mathbf{x})^T [K(\mathbf{x}, \mathbf{x}) + \sigma_N^2 I]^{-1} \mathbf{y} \quad (3)$$

$$\sigma(\mathbf{x}_*) = \frac{K(\mathbf{x}_*, \mathbf{x}_*) - K(\mathbf{x}_*, \mathbf{x})^T [K(\mathbf{x}, \mathbf{x}) + \sigma_N^2 I]^{-1} K(\mathbf{x}, \mathbf{x}_*)}{K(\mathbf{x}_*, \mathbf{x}_*)} \quad (4)$$

Here, the quantity $K(\mathbf{x}, \mathbf{x})$ is a square matrix with dimension $n \times n$ and the elements are $K(i, j) = (x_i, x_j)$. Therefore, the covariances between $\mathbf{y}(x_i)$ and $\mathbf{y}(x_j)$ are denoted by the matrix elements (x_i, x_j) , where K is a kernel function that depends on some parameters. The parameters of the kernel functions are found by maximizing the log marginal likelihood (LML) which is given by

$$\log p(\mathbf{y}|\mathbf{x}, \theta_3) = -\frac{1}{2} \mathbf{y}^T K^{-1} \mathbf{y} - \frac{1}{2} \log |K| - \frac{N}{2} \log(2\pi) \quad (5)$$

where $|K|$ is the determinant of K and θ_3 is the collective set of parameters for the analytical function of the kernel.

The quality of GP fit for a multidimensional surface depends on the kernel and the coordinate representation. In our fitting method, we used a Matérn kernel (M)¹⁵ having form

$$M(\mathbf{x}_i, \mathbf{x}_j) = \sum_{k=1}^6 \left[1 + \sqrt{5} l_k^{-1} |x_{i,k} - x_{j,k}| + \frac{5}{3} l_k^{-2} |x_{i,k} - x_{j,k}|^2 \right] \times \exp(-\sqrt{5} l_k^{-2} |x_{i,k} - x_{j,k}|^2) \quad (6)$$

Here, l_1 – l_6 are the characteristic length scales of Matérn kernel and are the parameters of θ_3 .

Grids Selection and Symmetrization of GP. In order to construct the training set for GP models, we construct a grid in Jacobi coordinates, using Latin hypercube sampling (LHS).¹⁶ We consider a grid where both of the monomer bond lengths (r_{13}, r_{24}) of CaF vary from $3.2 a_0$ to $7.5 a_0$ with $r_{24} > r_{13}$, the intermolecular separation R varies from $4.0 a_0$ to $20 a_0$, and the angles θ_1, θ_2 , and ϕ vary from 0 to π . We initially perform a RHF calculation on these random LHS grids. We discard those points for which the HF energy lies above a certain threshold, these points being regarded as irrelevant to the dynamics at ultralow collision energies. We use two criteria for the selection of the cutoff energy depending on the interparticle distances among the four atoms in Ca_2F_2 as described below:

1. When the CaF monomer bond length is smaller than $3.4 a_0$ and the bond length between two Ca atoms is less than $10 a_0$, we use the cutoff energy 4000 cm^{-1} to account for the repulsive barrier appropriately.
2. Otherwise, we consider a lower value of cutoff energy, 1000 cm^{-1} .

We perform the full *ab initio* electronic structure calculation on the resulting grid, using the RHF-CCSD(T) method described above. The *ab initio* points on these grids are calculated only for $r_{13} < r_{24}$, while the remaining surface is constructed according to symmetry considerations.

The procedure of symmetrization for the singlet potential of CaF–CaF is discussed in detail in our previous work.¹ Here, we discuss the symmetrization criteria briefly. The CaF–CaF surface must be symmetric either the exchange of two Ca nuclei or the exchange of the two F nuclei. This symmetrization procedure is accomplished by the exchange operators between two identical nuclei and a switching function. We define two functions $F_1(\vec{x})$ and $F_2(\vec{x})$ between which the switch is done:

$$F_m[u; m, w, F_1(\vec{x}), F_2(\vec{x})] = y(u, c, w) F_1(\vec{x}) + [1 - z(u, c, w)] F_2(\vec{x}) \quad (7)$$

where the sigmoid function y should be twice differentiable and switches within the finite interval $(c-w) < u < (c+w)$, and it is given by^{1,17}

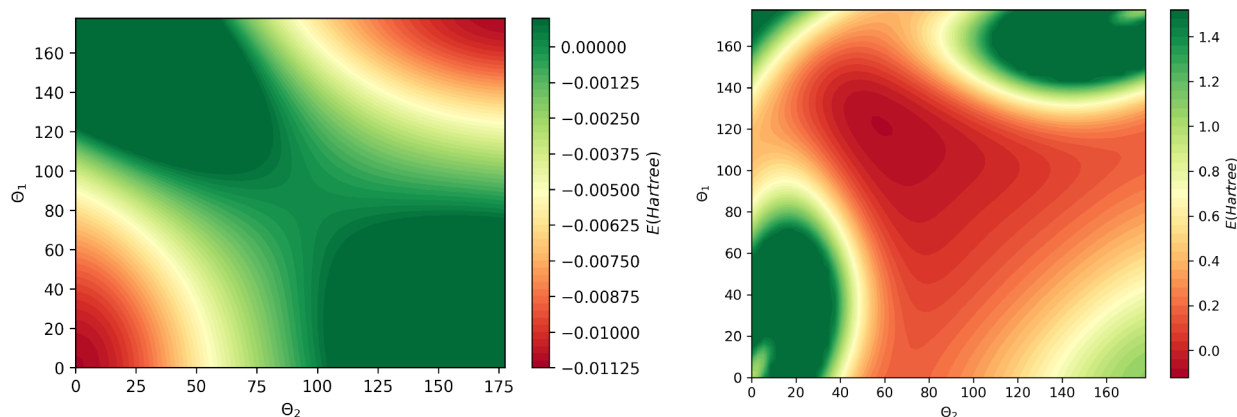
$$y(u, c, w) = \begin{cases} 0 & \text{if } u \leq c - w \\ \frac{1}{2} + \frac{9}{16} \sin \frac{\pi(u-c)}{2w} & \text{if } c - w < u < c + w \\ \frac{1}{2} + \frac{1}{16} \sin \frac{3\pi(u-c)}{2w} & \\ 1 & \text{if } u \geq c + w \end{cases}$$

Here, u is the parametrizing parameter for switching, c is the value of u around which the switch is centered and w is the half-width of the switching interval. Finally, the symmetrization scheme for the CaF–CaF arrangement is given by

$$V_1^{GP}(\vec{x}) = F_m \left[\frac{r_{13}}{r_{13} + r_{24}}; \frac{1}{2}, \frac{1}{16}, V^{GP}(\vec{x}), V^{GP}(\hat{P}_{12} \hat{P}_{34} \vec{x}) \right] \quad (8)$$

Table 4. Optimized Energy (cm^{-1}) and Bond Lengths (Bohr) of the Interpolated PES Ca_2F_2 for the Global and Local Minima

symmetry	r_{12}	r_{13}	r_{34}	r_{23}	r_{24}	r_{14}	E_{min}
D_{2h}	6.360	4.050	5.016				-18137
C_s	7.265	3.752	6.615	4.147	3.916	10.380	-8477

**Figure 3.** Variation of energy with respect to θ_1 and θ_2 in Jacobi coordinates, keeping other parameters remain constant. Left panel: $r_{13} = r_{14} = 3.7 a_0$, $R = 10$, $\phi = 180^\circ$. Right panel: $r_{13} = r_{24} = 4.05 a_0$, $R = 4.63 a_0$, $\phi = 180^\circ$.

$$V_2^{GP}(\vec{x}) = F_m \left[\frac{r_{23}}{r_{23} + r_{14}}; \frac{1}{2}, \frac{1}{16}, V^{GP}(\hat{P}_{12}\vec{x}), V^{GP}(\hat{P}_{34}\vec{x}) \right] \quad (9)$$

$$V_{\text{CaF-CaF}}^{GP}(\vec{x}) = F_m \left[\frac{r_{13} + r_{24}}{r_{13} + r_{24} + r_{23} + r_{14}}; \frac{1}{2}, \frac{1}{16}, V_1^{GP}(\vec{x}), V_2^{GP}(\vec{x}) \right] \quad (10)$$

where \hat{P}_{ij} are the exchange operators, which interchange the nuclei i and j . This symmetrization yields two advantages. First, symmetrization can reduce the configuration space over which we perform the GP fit, and second, the addition of the symmetrically equivalent points to the training set can improve the quality of the GP fit around the symmetrization boundaries.

RESULTS AND DISCUSSIONS

Construction of Training Set and Interpolation.

Following the algorithm above, we constructed a training data set based on the *ab initio* calculation for a total of 2075 atomic configurations. The coordinates of the grid points are transformed to inverse atomic distance coordinates. These coordinates are convenient, since it is difficult to describe different chemical arrangements of the four-body system equivalently by Jacobi coordinates making it is troublesome to fit the complete PES.¹ On the other hand, the GP fit works well everywhere on the surface exploiting inverse atomic distance coordinates.

Thereafter, we add symmetrically equivalent points to this *ab initio* data set, making a total number of grid points 3136 in the data set. We divide these points randomly into training and test sets, comprising 80% and 20% of the data, respectively. We fit the training set by GP regression. For this fitting, the kernel parameters of the Matérn kernel become [0.705, 0.74, 0.751, 0.749, 0.741, 1.08], the log marginal likelihood equal to 11190. The quality of the fit can be analyzed by computing the root-mean-square error of the interpolated data, with respect to the

test data set. This error of the fitting is on the order of 300 cm^{-1} , setting an approximate uncertainty of the fit. The interpolated potential appears on Github.¹⁸

As a second check, we find the minima of the interpolated surface, using a steepest-gradient-descent optimization method. The optimized results in terms of the energy and bond lengths are listed in Table 4. The optimized energy for these minima specifically for the global minimum is in agreement with the optimized results in MOLPRO with RHF-CCSD(T) calculation with an uncertainty approximately 100 cm^{-1} . This results indicate that the number of training points is sufficient for the construction of the triplet surface CaF–CaF.

As a further check, we present a contour diagram in Figure 3 in Jacobi coordinates to see the variation of energies for certain geometries. The purpose of these contour plots is to explore whether our GP model can reproduce the known results of the triplet surface of CaF–CaF obtained from MOLPRO. In the left-hand panel of Figure 3, we fix two monomer bond lengths (r_{13} and r_{24}) of each CaF at their equilibrium internuclear distance, two CaF molecules are separated by a distance $R = 10$ Bohr from the center of mass. Then we vary polar angles (θ_1 and θ_2) from 0 to 180° keeping the dihedral angle $\phi = 0$. The potential is minimum at the head-to-tail geometry, as expected.

In the right-hand panel of Figure 3, we fix $r_{13} = r_{24} = 4.05$ Bohr, $R = 4.63$ Bohr, $\phi = 180^\circ$, and we vary θ_1 and θ_2 from 0– 180° . The minimum energy shown is at the geometry $\theta_1 = 121^\circ$ and $\theta_2 = 59^\circ$, nearly coinciding with the result of the MOLPRO minimization.

Lifetime of the Collision Complex. A recent surprise in the field of ultracold molecular collisions is that the lifetime of the collision complex can be quite large. The simplest understanding of this is as follows. The four-body complex comprises a large phase space volume or equivalently, a high density of states ρ . If the number of open channels available for the complex to decay into is denoted N_ω , then a ready approximation for the lifetime of the complex is given by the RRKM expression

$$\tau = \frac{h\rho}{N_o} \quad (11)$$

where h is Planck's constant. In the case of ultracold molecules prepared initially in their ground state (an achievable situation these days), the number of open channels is only $N_o = 1$, often leading to estimated RRKM lifetimes of microseconds to milliseconds. In the case where lifetimes have been measured, they are sometimes even far larger, for reasons that remain mysterious. The current situation is reviewed in Bause et al.²

Given a potential energy surface such as our triplet potential, the density of states can be estimated by a quasi-classical calculation derived in ref 19. For a system having N_i particles, the total number of quantum states below a certain energy E , with total angular momentum J_0 and center of mass $\mathbf{X} = (0, 0, 0)$ is given by

$$N(E, J_0) = \frac{1}{h^{3N-3} \prod_i N_i!} \int d\mathbf{x} \int d\mathbf{p} \theta[E - H(\mathbf{x} - \mathbf{p})] \times \delta[\mathbf{P}(\mathbf{p})] \delta[\mathbf{X}(\mathbf{x})] \delta[J_0 - \mathbf{J}(\mathbf{x}, \mathbf{p})] \quad (12)$$

Here, $\theta(E)$ is the Heaviside step function, with $\theta(x) = 1$ for $x \geq 0$ and $\theta(x) = 0$ for $x < 0$. The factor $\prod_i N_i!$ is used to make correction for indistinguishability of the particles. The derivative of $N(E, J_0)$ with regard to energy E gives the DOS.

For the four-atom system, triplet CaF–CaF we use Jacobi coordinates which can be expressed as $\mathbf{q} = (r_{13}, r_{24}, R, \theta_1, \theta_2, \phi)$. The DOS in these coordinates can be expressed as¹⁹

$$\rho(E) = \frac{g_N 4\pi^6 (2J + 1) m_{\text{Ca}}^6 m_{\text{F}}^6}{h^9 (2m_{\text{Ca}} + 2m_{\text{F}})^3 g_{\text{Ca}_2\text{F}_2}} \int \frac{r_{13}^4 r_{24}^4 R^4 \sin^2(\theta_1) \sin^2(\theta_2)}{\det \mathcal{I}(\mathbf{q}) \sqrt{\det \mathcal{A}(\mathbf{q})}} [E - V(\mathbf{q})]^2 d\mathbf{q} \quad (13)$$

The term $g_{\text{Ca}_2\text{F}_2}$ is associated with degeneracy to account for indistinguishability, and g_N is a quantum mechanical factor which is defined as the fraction of classical phase space associated with parity. The masses of the atoms Ca and F are assigned as m_{Ca} and m_{F} , respectively. The explicit expressions for the terms $\mathcal{I}(\mathbf{q})$ and $\mathcal{A}(\mathbf{q})$ are given in Christianen et al.¹⁹

In the quasi-classical calculation of the DOS for the triplet potential energy surface of CaF–CaF, we choose an integration grid ranging from r_{13} (r_{24}) from $4a_0$ to $10a_0$ with a spacing of $0.3a_0$, and for R we use a grid of 71 points placed from $4a_0$ to $18a_0$. We use a 20-point Gauss–Legendre quadrature for θ_1 and θ_2 , and a 8-point Gauss–Chebyshev quadrature is used for ϕ between 0 to π . Note that, we use $r_{24} > r_{13}$ and multiply the result by a factor of 2 due to symmetry, and an additional 2 factor should be included for compensating ϕ for running up to π instead of 2π .¹⁹ Next, a geometry-dependent weighting factor needs to be assigned to the integrand, and this weighting factor $W(\mathbf{q})$ is deduced based on the symmetrization of the surface. For the triplet state arrangement of CaF–CaF, $W(\mathbf{q}) = W_1 W_2$, where the weighting factor $W(\mathbf{q})$ is equivalent to the function $\gamma(u, c, w)$ defined in the previous section. Here, $W_1 = W(u_1, 1, 1/4)$ with $u_1 = \frac{r_{12} + r_{34}}{2(r_{13} + r_{24})} + \frac{r_{12} + r_{34}}{2(r_{23} + r_{14})}$, and $W_2 = W(u_2, 1/2, 1/16)$ with $u_2 = \frac{r_{23} + r_{14}}{r_{13} + r_{24} + r_{23} + r_{14}}$.

Finally in Figure 4, we present the DOS as function energy $E - E_{\text{min}}$ in cm^{-1} , where E_{min} is energy of the minimum of the

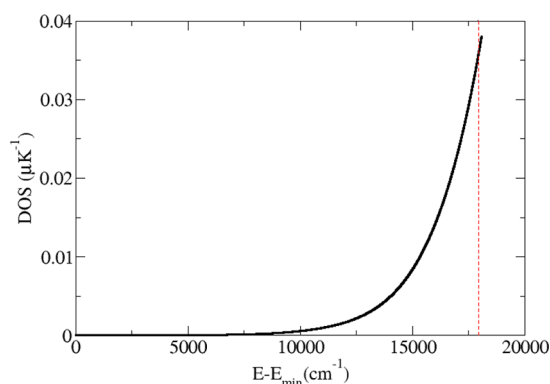


Figure 4. Density of state as a function of energy for the triplet CaF–CaF, the vertical dashed line indicates the dissociation threshold of the complex.

potential. The DOS is found to be $0.038 \mu\text{K}^{-1}$ near the dissociation energy for $J = 0$ in the field free case, and the corresponding RRKM sticking time of the collision complex is $1.8 \mu\text{s}$. Calculations are performed using the original code written by Christianen et al.,¹⁹ which is available on GitHub.²⁰

This lifetime is comparable to those associated with midsize alkali dimer complexes, such as KRb. The effect of sticking in these collisions is to temporarily remove molecules from an ultracold gas, as if they are reacting chemically, even when they are not. If the collisions take place in an optical dipole trap, then the complex may absorb a photon of the trapping light and be truly removed from the trap.

Even if this is not the case, a molecule such as CaF might be in danger. If the molecules remain in the triplet potential, then they may survive the complex and re-emerge as CaF molecules through the single open channel. However, if the molecules become stuck long enough in a collision complex in the triplet state, then they will have multiple opportunities during the lifetime of the complex to escape to the singlet surface by spin–orbit interactions, and hence complete the chemical reaction.

CONCLUSION

We constructed an *ab initio* potential energy surface of triplet CaF–CaF, followed by Gaussian process interpolation. The *ab initio* method used the CCSD(T)/cc-pwCVTZ-PP and aug-cc-PVTZ level of theory. The deduced potential was used to determine the DOS via quasi-classical calculations and subsequently used to determine the RRKM sticking time of $1.8 \mu\text{s}$ of the collision complex. The knowledge of the DOS, and RRKM lifetime would be useful to understand the loss mechanism of the complex.

AUTHOR INFORMATION

Corresponding Author

John L. Bohn – JILA, University of Colorado, Boulder, Colorado 80309, USA; Email: bohn@murphy.colorado.edu

Author

Bybendu Sardar – JILA, University of Colorado, Boulder, Colorado 80309, USA; orcid.org/0009-0008-5713-097X

Complete contact information is available at:
<https://pubs.acs.org/10.1021/acs.jpca.3c01676>

Notes

The authors declare no competing financial interest.

ACKNOWLEDGMENTS

We acknowledge funding from an AFOSR-MURI grant as grant number GG016303. D.S. especially acknowledges discussions with Kirk A. Peterson and Tijs Karman for *ab initio* calculations, and is thankful to Arthur Christianen for initial discussions about the Gaussian process regression.

REFERENCES

- (1) Sardar, D.; Christianen, A.; Li, H.; Bohn, J. L. Four-body singlet potential energy surface for reactions of calcium monofluoride. *arXiv*, Nov. 10, 2022, 2211.05909, ver. 1. <https://arxiv.org/pdf/2211.05909>.
- (2) Bause, R.; Christianen, A.; Schindewolf, I.; Bloch, I.; Luo, X.-Y. Ultracold sticky collisions: Theoretical and experimental status. *J. Phys. Chem. A* **2023**, *127*, 729.
- (3) Werner, H.-J.; Knowles, P. J.; Knizia, G.; Manby, F. R.; Schütz, M. Molpro: a general-purpose quantum chemistry program package. *Wiley Interdisciplinary Reviews: Computational Molecular Science* **2012**, *2*, 242–253.
- (4) Hill, J. G.; Peterson, K. A. Gaussian basis sets for use in correlated molecular calculations. XI. Pseudopotential-based and all-electron relativistic basis sets for alkali metal (K–Fr) and alkaline earth (Ca–Ra) elements. *J. Chem. Phys.* **2017**, *147*, 244106.
- (5) Lim, I. S.; Schwerdtfeger, P.; Metz, B.; Stoll, H. All-electron and relativistic pseudopotential studies for the group 1 element polarizabilities from K to element 119. *J. Chem. Phys.* **2005**, *122*, 104103.
- (6) Kendall, R. A.; Dunning, T. H., Jr; Harrison, R. J. Electron affinities of the first-row atoms revisited. Systematic basis sets and wave functions. *J. Chem. Phys.* **1992**, *96*, 6796–6806.
- (7) Hou, S.; Bernath, P. F. Line list for the ground state of CaF. *Journal of Quantitative Spectroscopy and Radiative Transfer* **2018**, *210*, 44–51.
- (8) Huber, K.; Herzberg, G. Constants of Diatomic Molecules. In *Molecular Spectra and Molecular Structure*; Van Nostrand, 1979; pp 8.
- (9) Meyer, E. R.; Bohn, J. L. Chemical pathways in ultracold reactions of SrF molecules. *Phys. Rev. A* **2011**, *83*, 032714.
- (10) Chen, E.; Wentworth, W. Negative ion states of the halogens. *J. Phys. Chem.* **1985**, *89*, 4099–4105.
- (11) Allard, O.; Samuelis, C.; Pashov, A.; Knöckel, H.; Tiemann, E. The European Physical Journal D-Atomic, Molecular. *Optical and Plasma Physics* **2003**, *26*, 155–164.
- (12) Balfour, W. J.; Whitlock, R. F. The visible absorption spectrum of diatomic calcium. *Can. J. Phys.* **1975**, *53*, 472–485.
- (13) Cui, J.; Krems, R. V. Gaussian process model for collision dynamics of complex molecules. *Physical review letters* **2015**, *115*, 073202.
- (14) Cui, J.; Krems, R. V. Efficient non-parametric fitting of potential energy surfaces for polyatomic molecules with Gaussian processes. *Journal of Physics B: Atomic, Molecular and Optical Physics* **2016**, *49*, 224001.
- (15) Williams, C. K.; Rasmussen, C. E. *Gaussian Processes for Machine Learning*; MIT Press: Cambridge, MA, 2006; Vol. 2.
- (16) Stein, M. Large sample properties of simulations using Latin hypercube sampling. *Technometrics* **1987**, *29*, 143–151.
- (17) Christianen, A.; Karman, T.; Vargas-Hernández, R. A.; Groenenboom, G. C.; Krems, R. V. Six-dimensional potential energy surface for NaK–NaK collisions: Gaussian process representation with correct asymptotic form. *J. Chem. Phys.* **2019**, *150*, 064106.
- (18) jila2021/Triplet-CaF-CaF, Mar. 4, 2023. <https://github.com/jila2021/Triplet-CaF-CaF>

(19) Christianen, A.; Karman, T.; Groenenboom, G. C. Quasiclassical method for calculating the density of states of ultracold collision complexes. *Phys. Rev. A* **2019**, *100*, 032708.

(20) Groenenboom, G. C. Efficient non-parametric fitting of potential energy surfaces for polyatomic molecules with Gaussian processes. Oct. 21, 2020. <https://gitlab.science.ru.nl/theochem/density-of-states>.

Recommended by ACS

Theoretical Study of Valence Shell Excitation by Electron Impact in CCl₄

Noboru Watanabe and Masahiko Takahashi

FEBRUARY 21, 2023
THE JOURNAL OF PHYSICAL CHEMISTRY A

READ 

CsAr, CsXe, and RbXe B²Σ_{1/2}⁺ Interatomic Potentials Determined from Absorption Spectra and Calculations of Franck–Condon Factors for Free–Free Optical Transition...

J. Darby Hewitt, J. Gary Eden, *et al.*

APRIL 12, 2023
THE JOURNAL OF PHYSICAL CHEMISTRY A

READ 

Toward Compact Selected Configuration Interaction Wave Functions with Quantum Monte Carlo—A Case Study of C₂

Jil Ludovicy, Arne Lüchow, *et al.*

MAY 02, 2023
JOURNAL OF CHEMICAL THEORY AND COMPUTATION

READ 

Plenty of Room on the Top: Pathways and Spectroscopic Signatures of Singlet Fission from Upper Singlet States

Yiting Bai, Maxim F. Gelin, *et al.*

NOVEMBER 23, 2022
THE JOURNAL OF PHYSICAL CHEMISTRY LETTERS

READ 

Get More Suggestions >